Real-Time and Offline Performance of Pattern Recognition Myoelectric Control Using a Generic Electrode Grid With Targeted Muscle Reinnervation Patients

Dennis C. Tkach, *Member, IEEE*, Aaron J. Young, *Student Member, IEEE*, Lauren H. Smith, Elliott J. Rouse, *Member, IEEE*, and Levi J. Hargrove, *Member, IEEE*

***Abstract*—Targeted muscle reinnervation (TMR) is a surgical technique that creates myoelectric prosthesis control sites for high-level amputees. The electromyographic (EMG) signal patterns provided by the reinnervated muscles are well-suited for pattern recognition control. Pattern recognition allows for control of a greater number of degrees of freedom (DOF) than the conventional, EMG amplitude-based approach. Previous pattern recognition studies have shown benefit in placing electrodes directly over the reinnervated muscles. Localizing the optimal TMR locations is inconvenient and time consuming. In this contribution, we demonstrate that a clinically practical grid arrangement of electrodes yields real-time control performance that is equivalent to, or better than, the site-specific electrode placement for simultaneous control of multiple DOFs using pattern recognition. Additional findings indicate that grid-like electrode arrangement yields significantly lower classification errors for classifiers with a large number of movement classes (>9). These findings suggest that a grid electrode arrangement can be effectively used to control a multi-DOF upper limb prosthesis while reducing the time and effort associated with fitting the prosthesis due to clinical localization of control sites on amputee patients.**

***Index Terms*—Electrode grid, electromyography (EMG) prosthesis control, pattern recognition, targeted muscle reinnervation, upper limb amputee.**

I. Introduction

Loss of an upper limb is a significant cause of disability that limits the functionality and quality of life of those affected. It has been estimated that there are over 41 000 major upper-limb amputees in the U.S. alone [1]. To date, the most common treatment for major upper-limb loss is a prosthesis. Neither body-powered nor electrically powered prostheses adequately restore the function of lost arms and both pose many challenges associated with comfort and usability. A key challenge for users of both types of devices, however, is achieving adequate control.

Typically, control of a myoelectric prosthesis is achieved by using the amplitude of the recorded EMG signal from a an antagonistic muscle pair to directly control the motor of the corresponding prosthesis joint [2]. This control strategy—referred to as direct control (DC)—is the most basic form of myoelectric prosthesis control and has gained clinical acceptance. A major shortcoming of DC is that for most patients, it cannot provide seamless transitions between the control of different DOFs. A limited number of independent EMG signal sources in most residual limbs [3] forces patients to use pressure sensing resistors or muscle cocontraction to switch modes between different DOFs. Use of alternative control algorithms such as pattern recognition (PR) enables seamless sequential control of multiple DOFs [4], [5] and furthermore, as our group has recently demonstrated, can be extended to classification of simultaneous activations of multiple DOFs [5]–[7]. PR algorithms interpret unique patterns of EMG signals recorded from multiple sites on the amputee's residual limb [5], [8], [9] to predict the movement(s) that the patient wishes to perform. PR control does not require independent muscle control sites that are free of crosstalk [8]. Furthermore, we have recently shown that PR control results in significant functional improvements over direct control when controlling physical prostheses [10].

In addition to alternative control algorithms, targeted muscle reinnervation (TMR) has further improved the accuracy and intuitiveness of myoelectric prosthesis control for patients with proximal amputations [11], [12]. TMR transfers nerves that originally innervated the amputated distal limb to muscles that are biomechanically nonfunctional after the amputation. Following the procedure, reinnervated muscles amplify the neural signals carried by the redirected nerves and EMG signals can be measured using surface electrodes [13]. A key outcome of TMR is that it establishes muscle control sites that can be independently activated in an intuitive manner by the amputee. When pairing TMR with PR control, the functional outcomes exceed those achieved with the TMR/DC combination [10], [14].

Manuscript received August 12, 2013; revised November 22, 2013; accepted December 12, 2013. Date of publication February 11, 2014; date of current version July 03, 2014. A. J. Young was supported by the National Science Foundation and NDSEG Graduate Research Fellowship 32CFR168a. L. H. Smith was supported by a Howard Hughes Medical Institute Research Fellowship.

D. C. Tkach is with the Center for Bionic Medicine at the Rehabilitation Institute of Chicago, Chicago, IL 60611 USA (e-mail: dtkach@ric.org).

A. J. Young and L. H. Smith are with the Center for Bionic Medicine at the Rehabilitation Institute of Chicago, Chicago, IL 60611 USA. They are also with the Department of Biomedical Engineering, Northwestern University, Chicago, IL 60611 USA (e-mail: ajyoung@u.northwestern.edu; lauren-smith@fsm.northwestern.edu).

E. J. Rouse is with the Department of Media Arts and Sciences, Massachusetts Institute of Technology, Cambridge, MA 02139 USA (e-mail: erouse@media.mit.edu).

L. J. Hargrove is with the Center for Bionic Medicine, Rehabilitation Institute of Chicago, Chicago IL 60611 USA. He is also with the Department of Physical Medicine and Rehabilitation, Northwestern University, Chicago, IL 60611 USA (e-mail: l-hargrove@northwestern.edu).

Digital Object Identifier 10.1109/TNSRE.2014.2302799

TABLE I
ADDITIONAL INFORMATION REGARDING STUDY SUBJECTS

Subject	Gender	Age	Amputation Type	Years Since Amputation	Years Since TMR
TH1	Female	44	Transhumeral	6	6
TH2	Male	34	Transhumeral	3	3
SD1	Female	32	Shoulder Disarticulation	7	7
SD2	Male	65	Shoulder Disarticulation	11	10

Clinical use of myoelectric prostheses with DC requires electrodes placed over muscles on the residual limb. Electrode placement is typically done through a repetitive and time-consuming process during which a clinician identifies electrode locations that minimize EMG crosstalk. However, because PR control does not require independent EMG signals [9], it should not require the added clinical burden of targeted electrode placement.

The use of nontargeted electrode placement for sequential DOF PR control has been previously evaluated by our group [10], [15], [16], as well as by others [17]. For transradial amputees, it was found that targeted electrode placement was not required to achieve low classification error rates; however, some benefit was found through targeted placement of electrodes over the reinnervated muscles for targeted muscle reinnervation patients [16]. Huang's analysis was completed by using adjacent, closely spaced electrodes in a high-density grid. We have recently shown that wider interelectrode spacing is beneficial for pattern recognition [18].

We hypothesized that using an electrode grid with wider interelectrode spacing than that previously used by Huang [16] may eliminate the need to target electrodes over the reinnervated muscles. In this paper, we compared a generic grid with large interelectrode spacing to targeted electrode placements based on clinical best practices for myoelectric control. This was tested using a variety of pattern recognition configurations—trained to recognize both discrete and simultaneous movements—offline and in real-time virtual tests.

II. METHODS

A. Data Collection

Four amputee subjects who have undergone TMR surgery following their amputation participated in this study (Table I). The reinnervation surgeries, described in [12], yielded control sites to control elbow flexion, elbow extension, hand opening, and hand closing when using a DC configured system. Each of the subjects is a user of a myoelectric prosthesis and is experienced in controlling the prosthesis via the conventional, DC approach. EMG signals were collected using self-adhesive, Ag/AgCl electrodes (Bio-Medical Instruments) with a 1-cm conductive area diameter.

The study consisted of two conditions: "Control Site" and "Grid". The two conditions were tested on two experimental sessions on separate days. In the "Control Site" condition, bipolar pairs of EMG electrodes were placed over each of the subject's muscle control sites, localized by palpation. Shoulder disarticulation subjects SD1 and SD2 had a total of 10 and 12 electrode pairs, respectively. Transhumeral subjects TH1 and TH2 had eight electrode pairs, each.

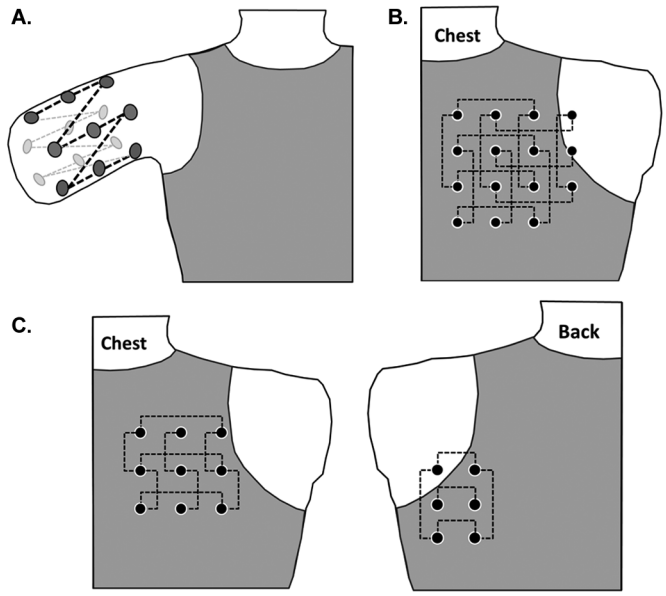

Fig. 1. Electrode placement configurations during Grid condition (a) Grid arrangement for TH subjects. Punctuated lines represent electrode pairs. Lighter circles represent electrodes on the posterior surface of the limb, while darker ones represent the anterior surface. (b) A 4 × 4 grid arrangement for subject SD1. (c) Split grid configuration for subject SD2. A 3 × 3 grid covers control sites on the subject's *pectoralis major* and *minor* muscles, while an additional 3 × 2 grid covers control sites on *serratus anterior* and residual *triceps brachii* muscle.

In the "Grid" condition, electrode pairs were arranged in a grid configuration either around the residual limb of the TH subjects [15] or along the surface of the chest of the SD subjects. The grid was arranged in a manner that provided complete and equidistant coverage [12] of each subject's control sites. Due to anatomic differences among subjects and the location of their respective control sites, grids were shaped differently for each subject. Despite the variable grid geometry, each grid was arranged such that electrode pairs maintained consistent interelectrode distance on a per subject basis and covered all of the subjects control sites.

For TH subjects, the grid was arranged as three rings of five electrodes [Fig. 1(a)]. Electrodes were paired to create 15 bipolar EMG channels. Pairings were organized along the long axis of the residual limb, connecting electrodes on adjacent rings with interelectrode distances ranging 30–60 mm. Ten electrode pairings were made in this manner. An additional five pairings were created by connecting electrode sites that were diagonally offset from each other with interelectrode distances ranging 80–100 mm.

For SD subjects, the grid was arranged in a planar fashion and placed over each subjects's torso to cover muscle control sites on their *pectoralis major, pectoralis minor*, and in the case of SD2, *serratus anterior* and residual *triceps brachii*. The precise configurations for each subject are shown in Fig. 1(b), (c). A total of 14 bipolar EMG channels were created for SD1 and a total of 15 bipolar EMG channels were created. Although the geometry of the grids varied for the SD subjects, functionally, the

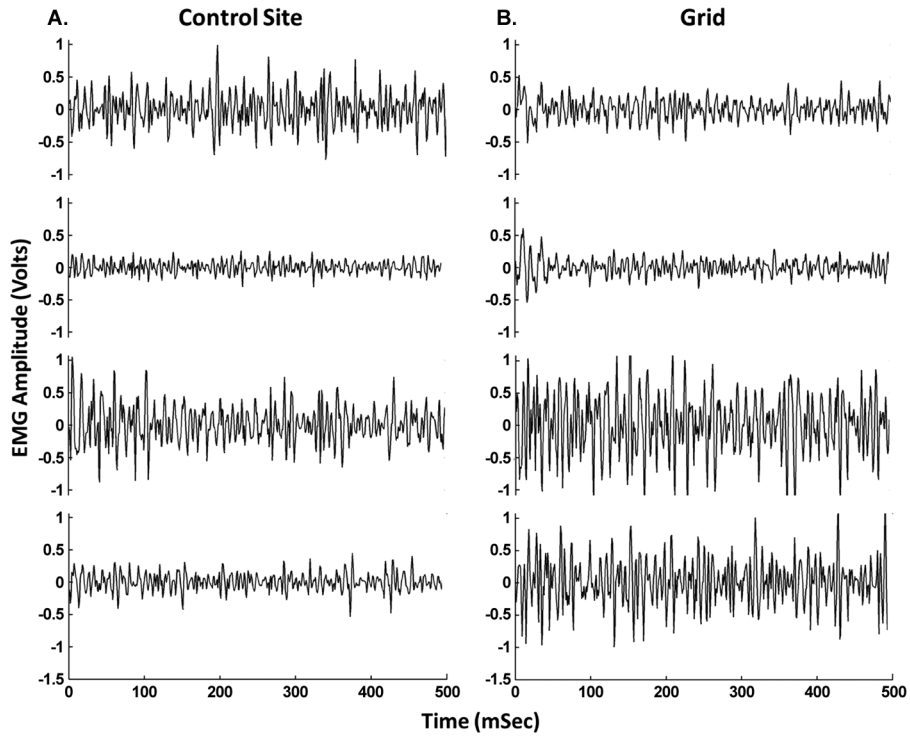

Fig. 2. Example EMG signals recorded from (A) Four Control sites and (B) four sites of the electrode grid during a combined motion of elbow flexion and hand closing (EF/HC). Shown data was recorded from subject SD1. Only 500 ms of a 3 s contraction are shown for visual clarity. The four grid channels shown correspond to the first four vertical bipolar electrode pairings from SD1's electrode grid, as seen in Fig. 1(b). 1st and 3rd EMG traces from the top in (A) correspond to Control sites that control elbow flexion and hand closure, respectively. 2nd and 4th EMG traces in (A) correspond to Control sites that control elbow extension and hand opening, respectively. Consequently, both are highly active during the combined motion contraction. Shown EMG data was band-pass filtered at 20–450 Hz using a second-order Butterworth filter.

grids were the same as they both provided adequate coverage of the subject's control sites with equidistant electrode placement.

During each experimental session (Control Site and Grid), EMG signals were recorded to train pattern classifiers for both online and offline analysis. Subjects were asked to execute a total of 29 different motions. Eight of these motions were discrete, single joint movements: *elbow flexion/extension*, *wrist flexion/extension*, *wrist pronation/supination* and *hand open/close*. Twenty of the motions were simultaneous activation of the eight discrete movements: (9–12) *elbow flexion/extension + hand open/close*; (13–16) *elbow flexion/extension + wrist flexion/extension*; (17–20) *elbow flexion/extension + supination/pronation*; (21–24) *wrist flexion/extension + hand open/close*; (25–28) *wrist supination/pronation + hand open/close*. The 29th motion class was a *no motion* condition, during which subjects maintained a relaxed posture. Subjects were prompted to perform the desired motions using a previously described screen training method [12]. Each motion was performed a total of four times for 3 s at a time. Representative EMG data recorded during a combined motion of *elbow flexion + hand close* by SD1 are shown in Fig. 2.

The recorded EMG signals were amplified by a gain of 4800×. Signals were digitally sampled using a custom 16-bit data acquisition system at 1 kHz and high-pass filtered at 20 Hz to reduce motion artifact. Acquired EMG data were segmented into 250 ms frames with a 50 ms frame increment [5], [19]. Time domain (TD) and autoregressive (AR) features were extracted from the EMG signals for use by pattern recognition algorithm [20]. The TD feature set included mean absolute value, zero crossings, slope sign changes, and waveform length. The AR feature set included the six coefficients of a 6th order autoregressive model, which was selected based on previous related work [21]. Linear discriminant analysis (LDA) was used for pattern recognition control (feature classification) because of its computational efficiency and its accuracy is comparable to other classification techniques [5].

B. Evaluation of Real-Time Controllability

The real-time controllability of the Control Site and the Grid conditions were evaluated in a virtual environment using: 1) a classifier providing the sequential control of discrete, single-joint motions and 2) a classifier providing simultaneous control of two DOFs. The first classifier (sequential real-time, denoted as "SeqRT") was trained to predict four single-joint motions (as well as the *no motion* class): *elbow flexion/extension* and *hand open/close* [6]. The second classifier (simultaneous real-time, denoted "SimRT") was trained to predict the *no movement* class, the four single-joint motions of SeqRT, and the following four combined motions classes: 1) *elbow flexion+hand open*; 2) *elbow flexion+hand close*; 3) *elbow extension+hand open*; 4) *elbow extension+hand close*. The real-time control for the Control Site and Grid experimental conditions was evaluated with each of the classifiers by the Target Achievement Control (TAC) test. The TAC test requires a subject to move a virtual limb from a nominal position to a target posture designated by a gray outline of the limb. Once the subject reaches the target

posture within the allowed 5 s and maintains it within a $\pm 15^{\circ}$ tolerance for 1 s, the target posture outline turns green and the trial is deemed a success. Full description of the TAC test is provided elsewhere [22].

Speed of the virtual limb movement was proportionally controlled based on the intensity of the muscle contraction [23], as measured by the mean absolute value of the EMG signals across all channels, normalized for each subject for a specific motion class. For motion classes involving simultaneous activation of two DOFs, a single speed was calculated for the motion class and assigned to the movement of both DOFs.

In addition to proportional speed control, we also imposed a decision-based velocity ramp on our controller to minimize the effect of unintended movements. The ramp functions by attenuating movement speed following a change in classifier decision [24]. A total of four TAC tests were performed per classifier type and per electrode arrangement type. A single TAC test consisted of a set single-DOF targets (elbow flexion/extension or hand open/close) and a set of dual-DOF targets (combinations of elbow and hand motion).

We evaluated controllability in the TAC test with three metrics: motion completion rate, motion completion time and length of movement error. Completion rate is defined as the percentage of total trials completed before a given time (5 s, in this case). Completion time is the time from movement initiation to the completion of the trial. Within-subject variability in the TAC test was evaluated by calculating the spread of completion times across trials. Length of movement error is defined as the length the subject's virtual limb has traveled beyond the total required distance, as a percentage of the total required distance. The total required distance is defined by the linear distance between the initial posture and the target posture, excluding any distance the subject may have traveled within the target posture

$$\text{Length error}(\%) = \frac{\text{(Distance Traveled-Optimal Distance)}}{\text{Optimal Distance.}}$$

As an example, a 100% length error would indicate that the subject's path length was twice the total required distance, while a 0% length error indicates that the subject traveled the minimum distance necessary to achieve the target posture.

C. Offline Evaluation of Classification Error

Classification error of the five motion class classifier (SeqRT) and the nine motion class classifier (SimRT) classifiers used during the real-time TAC tests was evaluated through offline analysis on the training data. Offline classification error was determined by performing a four-way cross validation analysis on the offline data used to train the classifier for real time control.

Offline classification analysis was further expanded to include a greater number of motion classes (not used for the real-time controllability tests). For this analysis five additional classifiers were created.

These five classifiers were tested across three conditions: the Control Site condition, the Grid condition, and a grid condition with a reduced set of EMG channels (Grid-Trim) to correspond with the number of channels used in the Control Site condition. For Grid-Trim, a random subset of channels was chosen from the full Grid, such that the number of channels was equal to the number of Control Site EMG channels. For each subject, subsets of grid channels were chosen randomly over 50 iterations. Resulting classification errors were averaged and represented performance of the Grid-Trim condition.

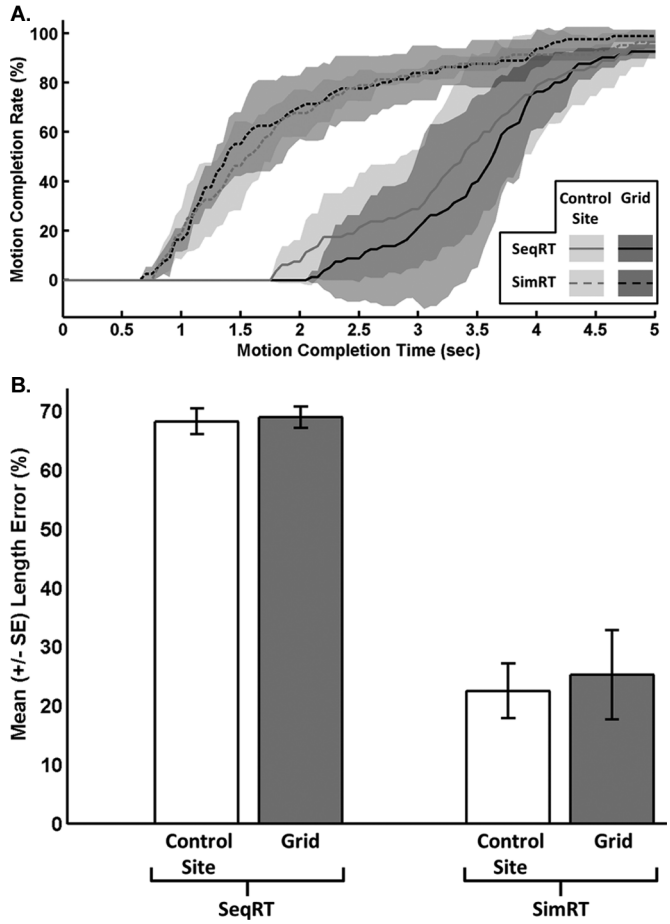

Fig. 3. Mean TAC test performance results across all subjects. (A) Motion completion rate curves for the Control Site (gray lines) and Grid (black lines) conditions showing performance of SeqRT (solid line) and SimRT (punctuated line) classifiers under each electrode placement configuration. Shaded areas around the lines represent ± 1 SE. (B) Average path length error percentages for the Control Site (white vertical bars) and Grid (gray vertical bars) conditions showing performance of SeqRT and SimRT classifiers under each electrode placement configuration. Error bars on each vertical bar represent ± 1 SE.

III. Results

A. Real-Time Functional Performance of Virtual Prosthesis Control

There was no difference in motion completion rates across subjects between the Control Site and Grid conditions (Fig. 3). This was true for both the SeqRT and SimRT classifiers ($p = 0.33$ and $p = 0.78$, respectively, two sample paired t-test). Average path errors were also unaffected by the configuration of the electrodes [Fig. 3(b)]. The mean path length error percentages for Control Site and Grid conditions with SeqRT classifier were 68.25% and 68.99%, respectively. These values were not statistically different from each other ($p = 0.8$, 2 sample paired t-test). The mean path length errors for Control Site and Grid electrode placements with SimRT classifier were 22.48% and

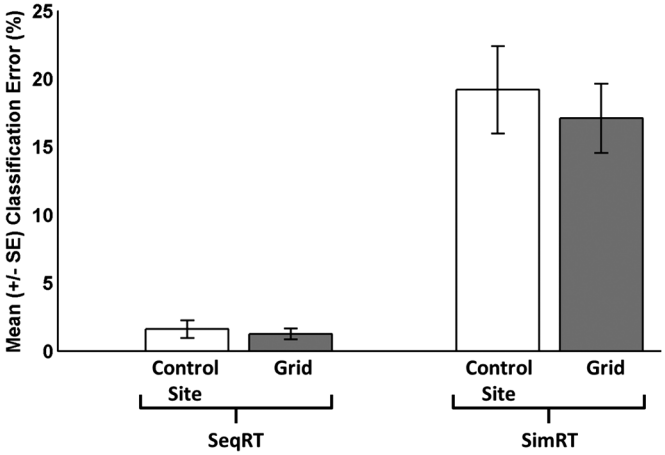

Fig. 4. Mean classification error of reconstructed SeqRT and SimRT classifiers across all subjects. Classification errors for the Control Site condition are shown as solid fill vertical white bars for SeqRT and as hashed fill white bars for SimRT. Classification errors for the Grid condition are shown as solid fill vertical gray bars for SeqRT and as hashed fill gray bars for SimRT. Error bars on each vertical bar represent ±1 SE.

25.25%, respectively. These values were also not statistically different from each other ($p = 0.77$, 2 sample paired t-test).

Table III displays the within-subject variability during the TAC test for each condition. There was no notable difference in the within-subject variability between the grid or control site conditions.

B. Offline Classification Error of Classifiers Used During Real-Time Controllability Tests

Consistent with the trend observed in the controllability of the virtual prosthesis, the mean classification errors of the reconstructed SeqRT and the SimRT classifiers were not significantly affected by the electrode placement configuration (Fig. 4). When using the SeqRT classifier, the mean classification errors for the Control Site and Grid conditions were 1.6% and 1.3%, respectively (±0.64 and 0.40 SE, respectively; $p = 0.65$, 2 sample paired t-test). Similarly, when using the SimRT classifier, the mean classification errors for the Control Site and Grid conditions were 19.2% and 17.1%, respectively (±3.20 and 2.53 SE, respectively; $p = 0.61$, 2 sample paired t-test).

C. Offline Classification Errors When Classifying Larger Sets of Motion Classes

Classification errors of the five classifier types (Table II) evaluated offline were sensitive to two factors: number of motion classes and the electrode arrangement (Fig. 5). A two-way ANOVA analysis ($f = 0.0035$) with *post hoc* comparisons (Bonferroni correction) indicated that classifiers with greater number of motion classes yielded higher classification errors than those with fewer motion classes. Classifiers with 17 motion classes each (*Seq, Elbow+Wrist* and *Seq, Wrist+Hand*) did not produce statistically different classification errors ($p > 0.5$).

Across all classifiers, classification errors resulting from the Grid-Trim analysis condition were higher than those from the

TABLE II
SETS OF MOTION CLASSES USED FOR OFFLINE COMPARISON OF GRID AND CONTROL SITE CONDITIONS

Classifier Name	Included Motion Classes*	# Motion Classes
Seq Only	Sequential elbow flex/extend, wrist pro/supinate, wrist flex/extend, hand open/close	9
Seq, Elbow+Hand	*Seq Only* classes and 4 combined motions: *elbow flex/extend+hand open/close*	13
Seq, Elbow+Wrist	*Seq Only* classes and 8 combined motions: *elbow flex/extend+wrist flex/extend, elbow flex/extend+wrist pro/supinate*	17
Seq, Wrist+Hand	*Seq Only* classes and 8 combined motions: *wrist flex/extend+hand open/close, wrist pro/supinate+hand open/close*	17
All	*Seq Only* classes and 20 combined motions: *elbow flex/extend+hand open/close, elbow flex/extend+wrist flex/extend, elbow flex/extend+wrist pro/supinate, wrist flex/extend+hand open/close, wrist pro/supinate+hand open/close*	29
*** In addition to the listed classes, all classifiers included the *no motion* class**		

TABLE III
WITHIN-SUBJECT VARIABILITY ON TAC TEST COMPLETION TIMES*

	SeqRT		SimRT	
Subject	**Control Site**	**Grid**	**Control Site**	**Grid**
TH1	2.90 ± 0.92	2.59 ± 0.60	1.49 ± 0.64	1.83 ± 1.40
TH2	4.19 ± 1.24	3.14 ± 1.32	1.91 ± 0.92	2.38 ± 2.60
SD1	3.94 ± 0.60	3.26 ± 0.56	1.69 ± 1.00	2.12 ± 0.92
SD2	3.89 ± 2.04	4.08 ± 0.52	1.88 ± 1.16	1.74 ± 1.20

*Completion time in seconds presented as mean and standard deviation

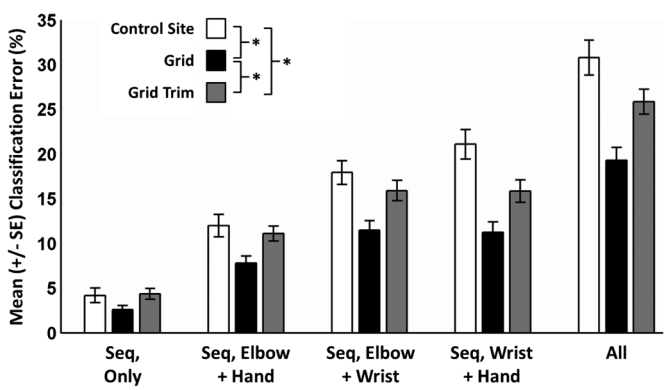

Fig. 5. Mean offline classification errors of classifiers with varying combinations of movement classes. Classification errors resulting from: Clinical Site electrode placement data are shown in white vertical bars; Grid electrode placement data are shown in black vertical bars; Grid Trim electrode selections are shown in gray vertical bars. Error bars represent ±1 SE. Statistically significant difference in the means of the data groups are denoted by vertical brackets and asterisks in the legend.

Grid condition ($p < 0.01$); however, they also remained significantly lower than the classification errors from the Control Site condition ($p < 0.01$).

The greatest discrepancy in the classification error between the Control Site and Grid conditions (11.47%) was evident for the *All* classifier, which consisted of 29 motion classes. The least discrepancy in the classification error between the Control Site and Grid conditions (1.69%) was evident when the least number of motion classes were trained. Classifiers *Seq, Elbow+Wrist*

and *Seq, Wrist+Hand* both consisted of 17 motion classes and under the Grid analysis condition both yielded similar classification errors of 11.5 ± 1.1% and 11.2 ± 1.2%. Under the Grid Trim condition the *Seq, Elbow+Wrist* and *Seq, Wrist+Hand* also produced nearly equivalent classification errors of 15.9 ± 1.1% and 15.8 ± 1.3%, respectively. Under the Control Site analysis condition, the two classifiers yielded higher errors of 17.9 ± 1.3% and 21.1 ± 1.7% respectively.

IV. Discussion

The current study demonstrates that a generic, grid-like electrode configuration can yield equivalent controllability and classification accuracy as precise placement of electrodes at muscle control sites in TMR patients. Furthermore, this study shows that both sequential DOF and simultaneous DOF real-time PR-based control can be achieved with a generic, grid-like placement of electrodes in TMR patients. These results have important implications for future clinical implementation of pattern recognition myoelectric control systems in TMR subjects.

The clinical process used for ideal placement of electrodes is referred to as "myotesting" and is a tedious and time-consuming process [25]. Myotesting is largely a trial and error procedure and often requires multiple visits to the prosthetic clinical. The process is even more difficult if restricted to a two channel EMG testing unit as are found in most prosthetic clinics. However, use of a generic electrode grid in a prosthesis socket eliminates the need for such a procedure, while maintaining the same levels of user performance. Although the grids used in this study were customized for each individual, a clinically viable method of incorporating such a grid has recently been proposed [26]. The Center for Bionic Medicine is now employing such a prefabricated, generic grid in a clinical trial of pattern recognition myoelectric control.

The equivalent performance of the electrode grid was evident for classifiers of relatively low complexity (Figs. 2, 3; SeqPR with five motion classes and SimPR with nine motion classes). We performed offline classification analyses to further examine the effect of electrode arrangement on classification error for classifiers with higher complexity than those used in real-time. The results of this analysis suggest that for classifiers with a greater number of motion classes (including those with simultaneous DOF movements) the grid-like arrangement of electrodes may outperform targeted electrode placement at muscle control sites (Fig. 5).

It is important to note that the number of EMG channel inputs into the classifiers differed between the Control Site and Grid experimental conditions. To ensure that the findings of our real-time and offline comparisons were not simply a consequence of the higher number inputs into the classifiers, we repeated our offline analysis with a reduced set of grid channels for each subject. In this analysis condition—Grid Trim—we restricted the number of grid channels to equal the number of channels in the Control Site condition for each subject. Although the classification errors from the reduced grid were higher than those from the full grid configuration, the reduced grid errors remained significantly lower than Control Site condition errors.

Our findings are in agreement with those from a study performed by Farrell *et al.* [17] on able-bodied subjects but differ from those presented by Huang *et al.* [16], which suggested that placing electrodes at muscle control sites yields higher classification accuracy than a geometric grid. The discrepancy in findings may be attributed to the fact that the configuration of the electrode grid in [16] was implemented differently from one used in this study. Huang *et al.* placed bipolar electrodes in an evenly spaced, geometric configuration, whereas our grid is comprised of evenly spaced electrode poles which were then paired longitudinally, laterally or diagonally to make bipolar EMG channels. Consequently, our grid arrangement included electrode poles connected across different muscle groups, as opposed to bipolar electrodes restricted to a single muscle group as in [16]. Recent work has demonstrated that including transverse electrode pairings along with the longitudinal and lateral pairs provides complimentary information to the PR EMG classifiers and reduces classification errors [18], [27]. It is possible that transverse pairings, in which the electrodes forming the bipolar pair are placed on two different muscles, record regularities in coordinated patterns between the muscles [28]. This coordinated activity would in turn lead to a much richer set of patterns and improved control, especially for simultaneous movements which require such coordination. Future work should further examine this hypothesis.

A notable limitation of this study was the small subject sample size $(\mathrm{N} = 4)$. Since TMR is a relatively recent procedure that continues to gain acceptance, the pool of TMR patients remains small, which limits the number of available TMR subjects. The four subjects included in this study were well suited to evaluate electrode placement configuration because they: 1) are accustomed to PR-based control; 2) have experience controlling multiple DOFs independently using clinical DC; and 3) have varying clinical locations of reinnervated control sites. They represent a fair sample of the relevant amputee population. The results of this study may also be applicable to non-TMR transradial amputees, as similar electrode grids may be used for sequential and simultaneous PR-based control.

Although the TMR subjects can control multiple DOFs independently using DC, the pattern recognition systems here offer advantages over the DC strategy. In closely related work by the authors [29], a comparison was made between simultaneous pattern recognition control using the non-grid configuration and conventional amplitude based control (or DC), using the same TMR subjects as in this study. The authors showed that simultaneous pattern recognition control improved all real-time TAC test performance metrics compared to the DC strategy. The average length error decreased from 92% to 27%, the average completion rate increased from 84% to 96%, and the average completion time decreased from 3.1 s to 2.0 s. These same metrics were used in this study to compare the grid and control site conditions. which demonstrated that simultaneous (and sequential) pattern recognition systems perform the same or better with the grid system. Thus this study, in combination with our related study [29], demonstrates that a generic grid configuration can perform the same as a targeted electrode placement (Fig. 3) for real-time control tasks for both sequential and simultaneous pattern recognition control and also demonstrate that both pattern

recognition systems outperform the conventional DC approach in real-time control tasks.

V. Conclusion

The main focus of this study was to compare a generic, grid-like electrode configuration to precise placement of electrodes at muscle control sites in TMR patients in terms of controllability in real-time and offline classification accuracy. Our results indicate that a generic grid performs as well or better than precise muscle targeting. These findings have significant implications as they offer a practical, cost effective means to increase upper-limb amputee patient access to myoelectric prostheses by greatly reducing the complexity and costs associated with fitting amputees with myoelectric devices.

Acknowledgment

The authors would like to thank the CBM electronics team, L. Miller, S. Finucane, and T. Kuiken, for providing project support and guidance.

References

[1] K. Ziegler-Graham, E. J. MacKenzie, P. L. Ephraim, T. G. Travison, and R. Brookmeyer, "Estimating the prevalence of limb loss in the United States: 2005 to 2050," *Arch. Phys. Medicine Rehab.*, vol. 89, pp. 422–429, Mar. 2008.

[2] M. Zecca, S. Micera, M. C. Carrozza, and P. Dario, "Control of multifunctional prosthetic hands by processing the electromyographic signal," *Critical Rev. Biomed. Eng.*, vol. 40, pp. 459–485, 2002.

[3] P. Parker, K. Englehart, and B. Hudgins, "Myoelectric signal processing for control of powered limb prostheses," *J. Electromyography Kinesiol.*, vol. 16, pp. 541–548, Dec. 2006.

[4] C. Alstrom, P. Herberts, and L. Korner, "Experience with Swedish multifunctional prosthetic hands controlled by pattern recognition of multiple myoelectric signals," *Int. Orthopedics*, vol. 5, pp. 15–21, 1981.

[5] K. Englehart and B. Hudgins, "A robust, real-time control scheme for multifunction myoelectric control," *IEEE Trans. Biomed. Eng.*, vol. 50, no. 7, pp. 848–854, Jul. 2003.

[6] A. Young, L. H. Smith, E. Rouse, and L. Hargrove, "A new hierarchical approach for simultaneous control of multi-joint powered prostheses," in *Proc. 4th IEEE RAS/EMBS Int. Conf. Biomedical Robotics Biomechatronics*, Rome, Italy, 2012.

[7] A. Young, L. Smith, E. Rouse, and L. Hargrove, Classification of simultaneous movements using surface emg pattern recognition 2012.

[8] L. Hargrove, K. Englehart, and B. Hudgins, "A comparison of surface and intramuscular myoelectric signal classification," *IEEE Trans. Biomed. Eng.*, vol. 54, no. 5, pp. 847–853, May 2007.

[9] T. R. Farrell and R. F. Weir, "A comparison of the effects of electrode implantation and targeting on pattern classification accuracy for prosthesis control," *IEEE Trans. Biomed. Eng.*, vol. 55, pp. 2198–2211, Sep. 2008.

[10] L. Hargrove, B. Lock, and A. Simon, "Pattern recognition control outperforms conventional myoelectric control in upper limb patients with targeted muscle reinnervation," in *Proc. 35th Int. Conf. IEEE Engineering in Medicine Biology Soc.*, Osaka, Japan, 2013.

[11] T. A. Kuiken, G. A. Dumanian, R. D. Lipschutz, L. A. Miller, and K. A. Stubblefield, "The use of targeted muscle reinnervation for improved myoelectric prosthesis control in a bilateral shoulder disarticulation amputee," *Prosthetics Orthotics Int.*, vol. 28, pp. 245–253, Dec. 2004.

[12] T. A. Kuiken, G. Li, B. A. Lock, R. D. Lipschutz, L. A. Miller, and K. A. Stubblefield *et al.*, "Targeted muscle reinnervation for real-time myoelectric control of multifunction artificial arms," *J. Am. Med. Assoc.*, vol. 301, pp. 619–628, Feb. 11, 2009.

[13] P. Zhou, M. M. Lowery, K. B. Englehart, H. Huang, G. Li, and L. Hargrove *et al.*, "Decoding a new neural-machine interface for control of artificial limbs," *J. Neurophysiol.*, vol. 98, pp. 2974–2982, Aug. 29, 2007.

[14] L. Hargrove, A. M. Simon, B. Lock, and T. A. Kuiken, "Pattern recognition control outperforms conventional control in upper limb patients with targeted muscle reinnervation," presented at the *American Academy of Orthotists Prosthetists 39th Academy Annual Meeting and Scientific Symp.*, Orlando, FL, USA, submitted for publication.

[15] D. Tkach, A. Young, L. H. Smith, and L. Hargrove, "Myoelectric control performance provided by generic electrode grid when used with targeted muscle reinnervation patients," in *Proc. 34th Int. Conf. IEEE Engineering Medicine and Biology Soc. (EMBS)*, San Diego, CA, USA, 2012.

[16] H. Huang, P. Zhou, G. Li, and T. A. Kuiken, "An analysis of EMG electrode configuration for targeted muscle reinnervation based neural machine interface," *IEEE Trans. Neural Syst. Rehab. Eng.*, vol. 16, no. 1, pp. 37–45, Jan. 2008.

[17] T. R. Farrell and R. F. Weir, "A comparison of the effects of electrode implantation and targeting on pattern classification accuracy for prosthesis control," *IEEE Trans. Biomed. Eng.*, vol. 55, no. 9, pp. 2198–2211, Sep. 2008.

[18] A. Young, L. Hargrove, and T. Kuiken, "Improving myoelectric pattern recognition robustness to electrode shift by changing interelectrode distance and electrode configuration," *IEEE Trans. Biomed. Eng.*, vol. 59, no. 4, pp. 645–652, Apr. 2012.

[19] L. H. Smith, L. J. Hargrove, B. A. Lock, and T. A. Kuiken, "Determining the optimal window length for pattern recognition-based myoelectric control: Balancing the competing effects of classification error and controller delay," *IEEE Trans. Neural Syst. Rehab. Eng.*, vol. 19, no. 2, pp. 186–192, Apr. 2011.

[20] B. Hudgins, P. Parker, and R. N. Scott, "A new strategy for multifunction myoelectric control," *IEEE Trans. Biomed. Eng.*, vol. 40, no. 1, pp. 82–94, Jan. 1993.

[21] Y. H. Huang, K. B. Englehart, B. Hudgins, and A. D. C. Chan, "A Gaussian mixture model based classification scheme for myoelectric control of powered upper limb prostheses," *IEEE Trans. Biomed. Eng.*, vol. 52, no. 9, pp. 1801–1811, Nov. 2005.

[22] A. Simon, L. Hargrove, B. A. Lock, and T. Kuiken, "Target achievement control test: Evaluating real-time myoelectric pattern-recognition control of multifunctional upper-limb prostheses," *J. Rehab. Res. Devel.*, vol. 18, pp. 619–628, 2011.

[23] L. Hargrove, P. Zhou, K. Englehart, and T. Kuiken, "The effect of ECG interference on pattern recognition based myoelectric control for targeted muscle reinnervated patients," *IEEE Trans. Biomed. Eng.*, vol. 56, no. 11, pp. 2197–2201, Nov. 2009.

[24] A. Simon, L. Hargrove, B. A. Lock, and T. Kuiken, "A decision-based velocity ramp for minimizing the effect of misclassifications during real-time pattern recognition control," *IEEE Trans. Biomed. Eng.*, vol. 58, no. 10, pp. 2360–2368, Oct. 2011.

[25] *Targeted Muscle Reinnervation: A Neural Interface for Artificial Limbs*. Boca Raton, FL, USA: Taylor and Francis, 2013.

[26] R. Lipschutz, B. Lock, D. Tkach, L. Hargrove, and T. Kuiken, "Systems and methods of myoelectric prosthesis control," U.S. Patent 20130046394, 2012.

[27] A. J. Young, L. J. Hargrove, and T. A. Kuiken, "The effects of electrode size and orientation on the sensitivity of myoelectric pattern recognition systems to electrode shift," *IEEE Trans. Biomed. Eng.*, vol. 58, no. 9, pp. 2537–2544, Sep. 2011.

[28] A. de Rugy, G. Loeb, and T. Carroll, "Muscle coordination is habitual rather than optimal," *J. Neurosci.*, vol. 32, pp. 7384–7391, 2012.

[29] A. Young, L. Smith, E. Rouse, and L. Hargrove, "A comparison of the real-time controllability of pattern recognition to conventional myoelectric control for discrete and simultaneous movements," *J. NeuroEngineering Rehab.*, 2013, submitted for publication.

Dennis C. Tkach (M' 11) received B.A. degrees in computer science and biology from Macalester College, St. Paul, MN, USA, in 2003, and the Ph.D. degree in computational neuroscience from the University of Chicago, Chicago, IL, USA, in 2009.

His early work focused on the development of brain-machine interfaces for upper-limb neuroprosthetic devices. In 2010, he joined the Center for Bionic Medicine (CBM), Rehabilitation Institute of Chicago, as a Research Scientist. During his tenure at CBM, he worked on the development of EMG-based neural control algorithms for use with upper and lower limb prosthetic devices, as well as managed the effort to commercialize a novel neural control interface system for transtibial amputees. In 2013, he joined the Center for Applied

Healthcare Studies (CAHS), VHA Inc., Irving, TX, USA, and currently leads the healthcare informatics, analytics and research efforts. His main areas of focus are evaluation of efficacy of emerging clinical technologies, reduction of hospital-borne harm to patients across U.S. hospitals, improvement in system-wide healthcare outcomes and reduction of costs to the health care system.

Dr. Tkach is a member of the Society for Neuroscience.

Aaron J. Young (S'11) received the B.S. degree from Purdue University, W. Lafayette, IN, USA, in 2009, and the M.S. degree in biomedical engineering from Northwestern University, Chicago, IL, USA, in 2011. He is currently working toward the Ph.D. degree at Northwestern University in the Center for Bionic Medicine at the Rehabilitation Institute of Chicago.

His research interests include neural signal processing and pattern recognition using advanced machine learning techniques for control of myoelectric prosthesis for the upper and lower limb.

Lauren H. Smith received the B.S. degree in biomedical engineering from Northwestern University, Evanston, IL, USA, in 2008. She is currently working toward both the M.D. and Ph.D. degrees in biomedical engineering at Northwestern University, Chicago, IL, USA.

Her research interests include neural interfaces, bioelectric signal analysis, and clinical neurophysiology.

Elliott J. Rouse (M'10) received the B.S. degree in mechanical engineering from The Ohio State University, Columbus, OH, USA, in 2007, the M.S. degree in biomedical engineering from Northwestern University, Evanston, IL, USA, in 2009, and the Ph.D. degree in biomedical engineering from Northwestern University in 2012, where he studied in the Center for Bionic Medicine.

He is currently a Postdoctoral Associate in the Biomechatronics Group, MIT Media Lab, Cambridge, MA, USA. His primary research interests include the design and control of wearable robotic technologies, biomechanics and system identification, culminating in the development of technologies to assist the disabled.

Levi J. Hargrove (S'05–M'08) received the B.Sc., M.Sc., and Ph.D. degrees in electrical engineering from the University of New Brunswick (UNB), Fredericton, NB, Canada, in 2003, 2005, and 2007, respectively.

He joined the Center for Bionic Medicine at the Rehabilitation Institute of Chicago, Chicago, IL, USA, in 2008. His research interests include pattern recognition, biological signal processing, and myoelectric control of powered prostheses.

Dr. Hargrove is a member of the Association of Professional Engineers and Geoscientists of New Brunswick. He is also a Research Assistant Professor in the Department of Physical Medicine and Rehabilitation (PM&R) and Biomedical Engineering, Northwestern University, Evanston, IL, USA.